Seeking sprite-induced signatures in remotely sensed middle atmosphere NO_2: latitude and time variations

Seeking sprite-induced signatures in remotely sensed middle atmosphere NO₂: latitude and time variations

E Arnone[1], **A Kero**[2], **C-F Enell**[2], **M Carlotti**[1], **Craig J Rodger**[3],
E Papandrea[1], **N F Arnold**[4], **B M Dinelli**[5], **M Ridolfi**[1] and **E Turunen**[2]

[1] Dipartimento di Chimica Fisica e Inorganica, Università di Bologna, Italy
[2] Sodankylä Geophysical Observatory, University of Oulu, Sodankylä, Finland
[3] Department of Physics, University of Otago, Dunedin, New Zealand
[4] Department of Physics and Astronomy, University of Leicester, Leicester, UK
[5] Istituto di Scienza dell'Atmosfera e del Clima – CNR, Bologna, Italy

E-mail: enrico.arnone@unibo.it

Abstract

Recent research on sprites shows these and other transient luminous events can exert a local impact on atmospheric chemistry, although with minor effects at global scales. In particular, both modelling and remote sensing work suggest perturbations to the background NO_x up to a few tens of per cent can occur above active sprite-producing thunderstorms. In this study we present a detailed investigation of MIPAS/ENVISAT satellite measurements of middle atmospheric NO_2 in regions of high likelihood of sprite occurrence during the period August to December 2003. As a proxy of sprite activity we used ground based WWLLN detections of large tropospheric thunderstorms. By investigating the sensitivity of the analysis to the characteristics of the adopted strategy, we confirm the indication of sprite-induced NO_2 enhancements of about 10% at 52 km height and tens of per cent at 60 km height immediately after thunderstorm activity, as previously reported by Arnone *et al* (2008b *Geophys. Res. Lett.* **35** 5807). A further analysis showed the enhancement to be dominated by the contribution from regions north of the Equator (5°N to 20°N) during the first 30 to 40 days of the sample (i.e. the tail of Northern Hemisphere summer) and in coincidence with low background winds.

(Some figures in this article are in colour only in the electronic version)
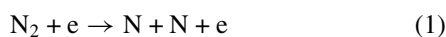
1. Introduction

Over the last two decades a whole family of upper atmosphere electrical discharges, collectively known as transient luminous events (TLEs), have been discovered and studied (e.g. Rodger (1999), Füllekrug *et al* (2006), Neubert *et al* (2008)). TLEs are produced by the electrical impact of thunderstorms on the above atmosphere, which causes ionization, dissociation and excitation of neutral air constituents (mainly N_2 and O_2) and the consequent well recognizable optical emissions. In analogy to other air plasma processes, TLEs perturb the chemistry of the atmosphere: the possibility of significant TLE contributions to the long-term atmospheric budgets and impact on stratospheric ozone have recently brought forward dedicated studies on TLE chemistry.

TLEs occur in the stratosphere–mesosphere region between the top of thunderclouds and the lower ionosphere, the height of occurrence determining both their nature and the chemical impact they may exert. Above thunderclouds, the formation of streamers (weakly ionized plasma channels) can occur roughly up to 70 km height above which the dielectric relaxation timescale becomes comparable to that of dissociative attachment leading to diffuse emissions (Pasko *et al* 1998). TLEs such as blue jets (Wescott *et al* 1995) and gigantic jets (Pasko *et al* 2002) are streamers directly injected from the thundercloud top towards the ionosphere and may be considered the upward equivalent

of cloud-to-ground (CG) lightning (Krehbiel *et al* 2008). Red sprites (Sentman *et al* 1995, Pasko 2007) are luminous discharges that initiate at about 70–80 km height, can extend downwards to 40 km as streamers and upwards to 90 km height as diffuse emission and be tens of kilometres wide. Sprite halos occur as diffuse emission around 70–80 km height (Barrington Leigh *et al* 2001). ELVES appear as horizontally expanding diffuse emission rings at the lower edge of the ionosphere (Fukunishi *et al* 1996). Depending on the relaxation timescales at the height of occurrence, TLEs last for a few hundred milliseconds (jets) down to milliseconds (ELVES), and are therefore to be considered as a transient compared with the much longer chemical and dynamical timescales typical of the upper atmosphere.

Sprites are the most commonly observed kind of TLE. They are generally produced by quasi-electrostatic electron heating induced by positive cloud-to-ground (+CG) lightning discharges (Pasko *et al* 1997). High-speed recording shows that the tendrils developing downwards from the ignition region at 70–80 km height are caused by fast moving ($\approx 10^7\,\mathrm{m\,s^{-1}}$) bright streamer heads followed by an almost static afterglow in their trails (McHarg *et al* 2007). Based on the interpretation of sprites as air plasma, four independent studies were published in 2008 for the first time modelling the ion–neutral chemistry in sprite-streamer heads and evaluating their chemical impact on the background atmosphere. Enell *et al* (2008), Sentman *et al* (2008), Gordillo-Vázquez (2008) estimated sprite-induced NO_x perturbations within streamer channels to be typically of the order of a few to a few tens of per cent between 50 and 80 km height (up to hundreds of per cent at 70 km height in extraordinary cases), with negligible ozone changes. Hiraki *et al* (2008) estimated orders of magnitude increases in NO_x and HO_x and significant ozone changes. The different initial conditions and reaction rates adopted may account for many of these differences. The models show that key reactions dominating the NO production in the height range 60–70 km are electron impact on N_2

$$N_2 + e \rightarrow N + N + e \tag{1}$$

with atomic N being either in its ground (^{4}S) state or in its (^{2}D) state, and consequent N oxidation

$$N(^2D) + O_2 \rightarrow NO + O \tag{2}$$
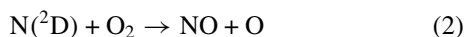
with atomic O either in the ground or (^{1}D) state, together with minor contributions from ion species in the first 1–10 s (Sentman *et al* 2008). The production of NO depends on the branching ratio of equation (1) into $N(^2D)$, while NO destruction on the branching into $N(^4S)$. The main reaction that could lead to reconversion of NO into N_2 (N + NO $\rightarrow$ N_2 + O) is slower than diffusion timescales so that the NO produced can be diffused away before being destroyed. On timescales of 10^2–10^3 s, NO is completely converted into NO_2 through reactions with O_3, O and HO_2, with the final production step NO_2 lasting hours (Hiraki *et al* 2008).

Two recent observational studies investigated sprite-induced chemical changes using middle atmosphere satellite

measurements. Arnone *et al* (2008b, hereafter paper I) found a probable sprite-induced NO_2 perturbation of 10% at 52 km height and of tens of per cent at 60 km height in coincidence with active thunderstorms, and no evident sprite global impact. Using a climatological approach, the multi-year study by Rodger *et al* (2008) concluded that sprites and other TLEs occurring below 70 km altitude do not exert a significant impact on the neutral chemistry at a global scale. Even though paper I made use of first-order backward trajectories to locally account for transport by winds, neither of the studies modelled the effect of overall transport in their global approaches so that a TLE-component in the global zonally averaged NO_x may still exist. The height of occurrence of TLEs covers the stratospheric ozone layer, which is regulated by the NO_x and HO_x families, and acts as a driver of the upper atmosphere together with momentum deposition by wave breaking (see, e.g., Brasseur and Solomon (2005)). Even though not directly impacting the radiative/dynamics balance of the upper atmosphere, TLE-NO_x production should be compared with known sources due to oxidation of tropospheric N_2O and energetic particle precipitation (e.g. Callis *et al* (2002), Funke *et al* (2005a)) since a large fraction of middle atmospheric air is processed by TLEs over the years.

The merging of the modelled chemical impact within streamers and the observed regional impact into a consistent overall scenario has to date been prevented by the lack of multi-scale multi-streamer modelling, although a few examples of order of magnitude comparisons have been attempted by Enell *et al* (2008) and Hiraki *et al* (2008). With the aim of better constraining the characteristics of sprite-induced chemical changes, we further analysed the data used in paper I, and present in this study the details of the dependence of the results on geolocation, time and adopted parameters. The investigation was based on measurements of nighttime NO_2 from the Michelson interferometer for passive atmospheric sounding (MIPAS) retrieved with a two-dimensional tomographic approach, so as to enhance the sensitivity of detecting small variations. Regions with a high likelihood of sprite occurrence were identified using measurements from the World Wide Lightning Location Network (WWLLN). We describe the data we analysed in section 2 and the adopted methodology in section 3. Results are discussed in section 4, together with an analysis of the sensitivity of the results on geolocation, time and adopted parameters. Conclusions are given in section 5.

2. Data

2.1. Measurements of middle atmospheric NO_2

We used NO_2 measurements from the MIPAS (Fischer *et al* 2008) instrument on board the European Space Agency (ESA) ENVIronmental SATellite (ENVISAT). MIPAS is a limb-scanning Fourier transform spectrometer recording emission of the atmosphere in the mid-infrared (680–2410 cm^{-1}). The spectra analysed in this work were taken with spectral resolution of 0.035 cm^{-1} FWHM,

unapodized. Global coverage is assured by 14.3 daily quasi-polar orbits, running at 10:00 am and 10:00 pm local time. In the adopted observation mode one orbit consists of 72 backward-looking limb-scans, each scan recording 17 observation geometries with tangent altitudes between 6 and 68 km. The instantaneous field of view (IFOV) of MIPAS is about 3 km in height at tangent point and 30 km wide (i.e. along longitude). In latitude, along the line of sight crossing the atmosphere below 80 km, the IFOV footprint is about 1200 km at 52 km height and 500 km at 60 km height.

NO$_2$ was retrieved adopting the geo-fit multi-target retrieval (GMTR) algorithm (Carlotti *et al* 2006) version 1.03 with no optimal estimation or regularization. NO$_2$ was obtained at the end of a retrieval cascade then exploiting the atmospheric fields previously derived for all atmospheric main targets. A multi-target retrieval was operated for pressure, temperature, water vapour and ozone. Unlike common one-dimensional methods, GMTR performs a two-dimensional tomographic retrieval of a whole orbit that makes it possible to model the horizontal inhomogeneity of the atmosphere. The GMTR approach can resolve horizontal structures (as expected crossing a region of sprite-induced NO$_2$ enhancements) by fitting simultaneously all lines of sight that cross the target regions recorded during successive satellite scans (Carlotti *et al* 2001), in contrast to one-dimensional retrievals that assume horizontal homogeneity of the atmosphere. Because of the two-dimensional discretization of the atmosphere adopted by the GMTR, the geometrical heights of the retrieval are fixed for all measurements. This retrieval method provided random errors for NO$_2$ of about 0.5 ppbv (about 5%) in volume mixing ratio (VMR) at 52 km. Systematic errors on NO$_2$ are about 20% at 52 km. However, the use of NO$_2$ anomalies (i.e. $\Delta NO_2 = NO_2 - \langle NO_2 \rangle$) we made in this study makes our results dependent on random errors but not on systematic errors.

Even though NO is the main expected sprite production, we used nighttime NO$_2$ as a proxy of NO$_x$: in fact, at night NO is converted into NO$_2$ within minutes and perturbations to its concentration are expected to last hours in the absence of solar radiation (see Hiraki *et al* (2008)). Moreover, middle atmospheric NO is strongly affected by non-local thermodynamic equilibrium (non-LTE), i.e. deviation of rotational and vibrational temperatures from the kinetic temperature (see Funke *et al* (2005b) and references therein), a deviation which is not modelled in the GMTR algorithm. Furthermore, non-LTE is the dominant component of the systematic error affecting NO$_2$ above 50–60 km height, causing underestimation of the retrieved NO$_2$ by up to 30% (Funke *et al* 2005b). Non-LTE is not considered also by the aforementioned sprite-streamer models, although it could be important since the integrated brightness of non-LTE afterglow emissions in the sprite trails may even exceed that modelled in streamer heads (Sentman *et al* 2008). If, on the one hand, non-LTE deviations can be accounted for as a moderate underestimation in the retrieval of the overall NO$_2$ observed minutes after the events, on the other hand non-LTE will have to be considered when attempting to fully model the chemical impact of sprites and in order to find direct evidence of sprite emissions. See section 4.4 for further discussion.

2.2. Localization of thunderstorm activity

As a proxy of sprite occurrence we used thunderstorm activity localized through lightning detections from the WWLLN (Rodger *et al* (2006) and references therein). Thunderstorm activity is mainly confined within the tropics, over the continents and continental coasts (see e.g. Williams (1992), Christian *et al* (2003)), with hot spots of very high lightning occurrence over South America, Central Africa and South East Asia. The first global TLE occurrence distribution from the ISUAL satellite (Chen *et al* 2008) shows that sprites and gigantic jets tend only partly to follow these chimneys, displaying hot spots of high occurrence also over the Japan Sea and West Atlantic Ocean, consistently with thunderstorm activity transported by wind (Christian *et al* 2003) over the sea where the likelihood of +CG occurrence is higher.

The WWLLN network exploits the electromagnetic power radiated into the very low frequency radio band (3–30 kHz) by strong lightning discharges. These radio pulses can be detected thousands of kilometres from the source. The current (December 2008) configuration of 32 stations allows close to global coverage, with discharge location and timing provided through combining observations from at least four receiving stations. At this stage WWLLN detects only a few per cent of the lightning strokes globally, corresponding to those with the largest peak currents. Even though a direct correlation with sprites would require information about the polarity and the charge moment of the lightning discharges, the adopted proxy is able to identify regions with active thunderstorms, and thus with a high likelihood of sprite activity. In fact, WWLLN was shown to detect nearly all lightning producing storms (Jacobson *et al* 2006). For the time period of our MIPAS-WWLLN comparison, WWLLN consisted of 11 stations, with a global detection efficiency of 1% which was strongly biased towards South East Asia and Northern Australia, and away from the strong chimney regions in central Africa and the Americas.

Additional information on the location of sprite-producing thunderstorms may be found inspecting cloud-top temperatures in IR images (see, e.g., São Sabbas and Sentman (2003)), so as to reduce the number of spurious correlations included in this study. The use of extremely low frequency (ELF) radio data to obtain information on the polarity of the lightning strokes is also foreseen, although the poor spatial accuracy of ELF makes their use in a global study of one-to-one correlations very difficult.

It should be noted that the use of 10:00 pm NO$_2$ measurements is not ideal considering sprites typically occur at the late stages of thunderstorms (Lyons 2006) which may be delayed well into the night. However, outside, e.g. the US High Plains hot spot not treated in this analysis, sprites are indeed detected also in the period from sunset to 10:00 pm (see, e.g. the EuroSprite campaign 2008—http://www.eurosprite.net). The 10:00 pm measurement time should be considered in extrapolating the results of this study to global properties since different parts of the globe may have a different sprite occurrence peak-time. A similar bias induced by the time of measurement affects also satellite imaging detections (see, e.g., ISUAL—Chen *et al* (2008), observing at 10:30 to 11:20 pm).

3. Methodology and data analysis

The correlation between MIPAS/GMTR nighttime NO_2 and WWLLN thunderstorm detections was studied in the period August to December 2003, for which both datasets were available and of sufficient quality. We correlated MIPAS measurements and intense lightning activity by integrating the number of WWLLN lightning strokes recorded within a coincidence window. The window was shaped according to the MIPAS IFOV footprint and located around the geolocation of the NO_2 measurement; we adopted a $30\,km \times 500\,km$ and a $60\,km \times 500\,km$ footprint, the latter being twice as wide along longitude as the actual MIPAS IFOV. A series of time intervals was adopted for the coincidence window, ranging from 10 to 120 min prior to the NO_2 observation. A NO_2 measurement was considered in coincidence with intense thunderstorm activity (and thus high likelihood of sprite activity) if the integrated number of WWLLN lightning strokes passed a threshold events per coincidence window. The threshold was varied from 1 to 50.

A series of combinations of sizes, time intervals of the window and lightning flash thresholds were investigated, leading to an optimized reference scenario of $60\,km \times 500\,km$, 60 min and 10 WWLLN detected lightning flashes (details are given in section 4). Because of the low statistics considered in studying individual bands, transport due to horizontal winds was accounted for by adopting the larger size of the coincidence shape (60 km wide) rather than introducing backward trajectories. Therefore, all coincidences should be considered as a 'static' correlation (i.e. the coincidence window is not moved during the integration time—see paper I for details). Given the 1% WWLLN efficiency, the adoption of a threshold of 10 WWLLN detections implies that we are considering only regions of very intense lightning activity, roughly of the order of 1000 lightning strokes per hour. We adopt the label WWLLN-NO_2 for the NO_2 measurements that fall within the coincidence window with WWLLN measurements, so as to distinguish them from background NO_2 (i.e. all available nighttime NO_2 measurements). The reader should note that since we have information only about where lightning occurred through the patchy 2003 WWLLN observations (and not about where lightning did not occur) we cannot discriminate clear sky background NO_2 and thus consider conservatively all available measurements (including WWLLN-NO_2) as background NO_2. This is a reasonable approach since generally any thunderstorm generated effect will average out over the many more clear sky observations.

In order to minimize the effects of the strong latitude variations observed in the distribution of NO_2, we considered NO_2 measurements over narrow latitude bands of $5°$ (MIPAS latitudinal resolution). The time series of MIPAS NO_2 measurements within each selected band were detrended using a 100-satellite-passes running mean, which roughly corresponds to a one-week-smoothed trend. The detrending process removed the dependence on the systematic errors affecting the retrieved absolute values and the seasonal variations of NO_2. The NO_2 measurements were then studied as anomalies (ΔNO_2), i.e. differences with respect to the running mean. We define as positive (negative) the ΔNO_2 above (below) zero, i.e. NO_2 measurements larger (smaller) than the local background.

4. Results and discussion

In paper I, NO_2 anomalies calculated over individual bands were joined into an overall distribution in order to have larger statistics and enhance our capability of detecting any possible deviation of WWLLN-NO_2 compared with background NO_2. The distribution of local WWLLN-NO_2 anomalies showed a perturbation of about 10% at 52 km and tens of per cent at 60 km height compared with the distribution of background anomalies.

In order to trace back the regions that provide the dominant contribution to the perturbation of the overall distribution reported in paper I, in this study we analyzed individual $5°$ latitude bands and the relationship between individual measurements and relevant parameters.

Constraints to the MIPAS NO_2 measurements that can be used during the analyzed period are imposed by the strong seasonal variability of NO_2 and by the seasonal changes of mid-atmospheric wind jets. In the time period considered, seasonal changes and shorter term variability of NO_2 at mid- to high latitude exceed a factor of 10 especially due to downward transport of mesospheric air in the winter hemispheres and during the October 2003 *Halloween* solar proton and electron precipitation events (e.g. Funke *et al* (2005a), Seppälä *et al* (2007)), thus making possibly tens of per cent sprite perturbations undetectable. These constraints are visible in the zonal mean VMRs of NO_2 in August and November 2003 shown in figure 1. On the other hand, strong zonal winds of up to $100\,m\,s^{-1}$ affected the middle atmosphere south of about $30°S$ up to day 280 of 2003, and north of about $30°N$ after day 300 of 2003 (see figure 2 for average zonal winds from the European Centre for Medium-Range Weather Forecasts—ECMWF). Even adopting backward trajectories to account for zonal transport induced by zonal winds, at these high wind speeds it would be impossible to perform any meaningful correlation between sprite emitted NO_2 and observed NO_2 at the time of measurement: after only 30 min, emitted sprite-NO_2 would be displaced by 180 km, i.e. 6 times MIPAS IFOV footprint along longitude and along random local trajectories.

Focusing on the tropics, the expectation is of high lightning/high sprite activity regions, although at the cost of excluding, for example, the United States where a large number of sprite-producing thunderstorms are known to occur (see, e.g., the large sprite-producing thunderstorms over the US High Plains reported by Lyons (2006)). The height of 52 km was chosen as the best compromise between any possible sprite signature (above 50 km height) and the quality of MIPAS data (which degrades above 60 km height). As shown in figure 1, the selected height/latitude region (52–60 km height and $-30°$–$20°$ latitude) has on average low values of NO_2 so that perturbations can be easily detected.

Figure 3 reproduced from paper I shows the global distribution of NO_2 at 52 km altitude in the period August to
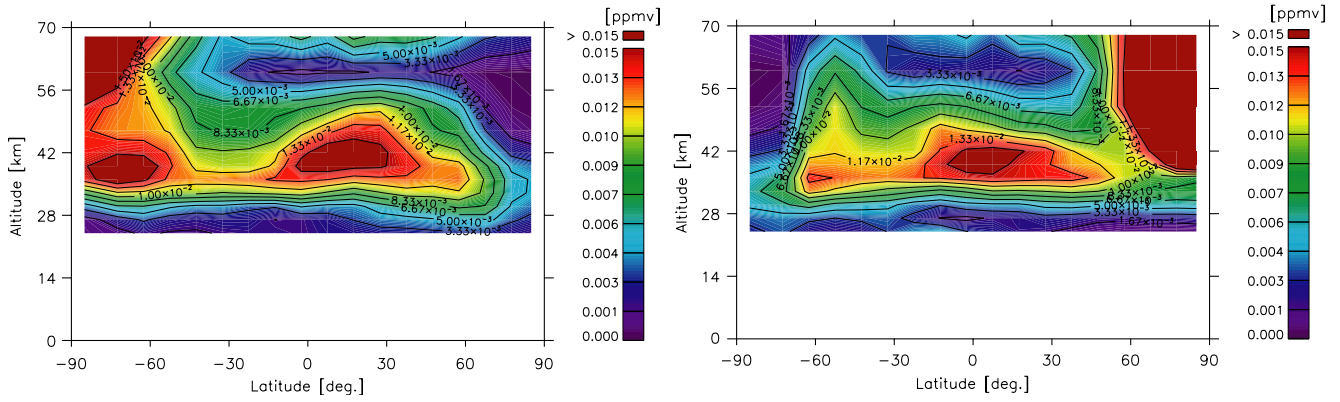
Figure 1. Monthly zonal mean nighttime NO_2 from MIPAS/GMTR for August (left) and November 2003 (right).
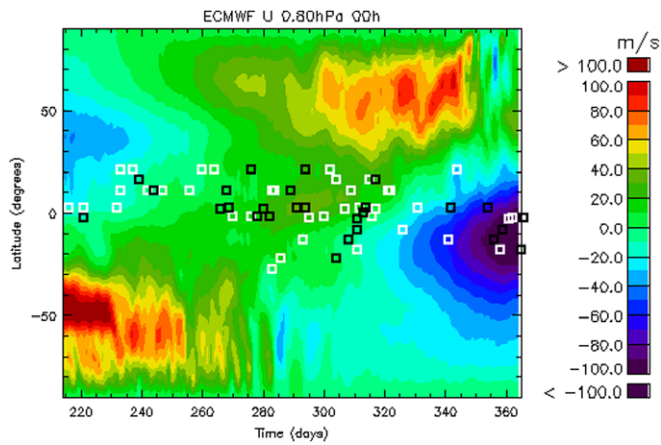

Figure 2. ECMWF daily mean zonal winds at 0.80 hPa (approximately 50 km height) for the period considered in the analysis. The time axis is in days of 2003. Squares indicate WWLLN-NO_2 coincidences, having a positive (white) or negative (black) NO_2 anomaly. See section 4.1 for details.

Figure 3. Mean nighttime NO_2 at 52 km height by MIPAS (*a*) and WWLLN lightning activity ((*b*): black = detections between 21 and 22 local time; red = WWLLN-MIPAS coincidences) for the period August to December 2003. From Arnone *et al* (2008b).

December 2003 (panel a) and WWLLN lightning detections over the same period (panel b). There is no evidence in the figure (or over shorter time periods, not shown) of a correlation of the time-average NO_2 with high lightning activity, e.g. over land and/or in correspondence with the overall WWLLN detections. This is consistent with the findings of Rodger *et al* (2008). Red dots in figure 3 indicate the locations of WWLLN-NO_2 that are discussed over individual latitude bands in the following section.

4.1. NO_2 anomalies over narrow latitude bands

Figure 4 shows the results of the analysis performed for nighttime NO_2 at 52 km over 5° latitude bands adopting the reference scenario, i.e. a coincidence window with a 60 km × 500 km footprint, 60 min period and 10 lightning flashes threshold (see section 3). Panels in the left column report the time series of background nighttime ΔNO_2 (black) over the four latitude bands that had sufficient coincidences, i.e. 15°N–20°N, 5°N–10°N, Equator–5°N and 5°S–Equator (top to bottom). The further bands down to 30°S–25°S, as well as the band 10°N–15°N, led to only up to four coincidences each and are thus not shown. Superimposed coloured squares indicate
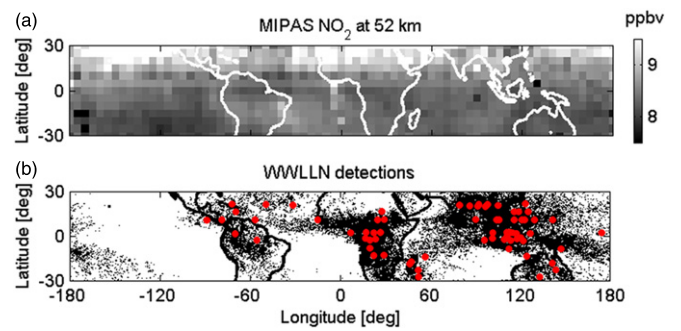
WWLLN-NO_2 coincidences: positive ΔNO_2 are marked in red and negative ΔNO_2 in blue. The second panel from the top of the figure corresponds to the case reported in figure 2 of paper I (note that a refinement in the data filtering led to minor changes).

The time series of background ΔNO_2 consists of all available MIPAS measurements over individual latitude bands, consistently counting between 1230 and 1556 MIPAS measurements. Given the strict selection criteria adopted, background conditions in NO_2 are homogeneous, with average absolute values (not shown) around 10 ppbv and standard deviation about the running mean of 1.5–2.2 ppbv depending on the latitude band. Random errors on a single measurement are about 0.5 ppbv (5%). The homogeneity of background conditions is evident from the distribution of background ΔNO_2 (black) reported in the right column of figure 4, each corresponding to the respective latitude band in the left column. The need for the latitude constraints (30°S–20°N) imposed by the high NO_2 variability is visible as a tendency of increasing scatter occurring after day 300 of the northern bands and over the first weeks in the southern bands (not shown).

Unfortunately, the WWLLN-NO_2 coincidences are not homogeneously distributed, with only four latitude bands having more than 10 WWLLN-NO_2 (bands 15°N–20°N, 5°N–10°N, Equator–5°N and 5°S–Equator, figure 4 (top to bottom), having, respectively, 10, 15, 15 and 14 WWLLN-NO_2) in
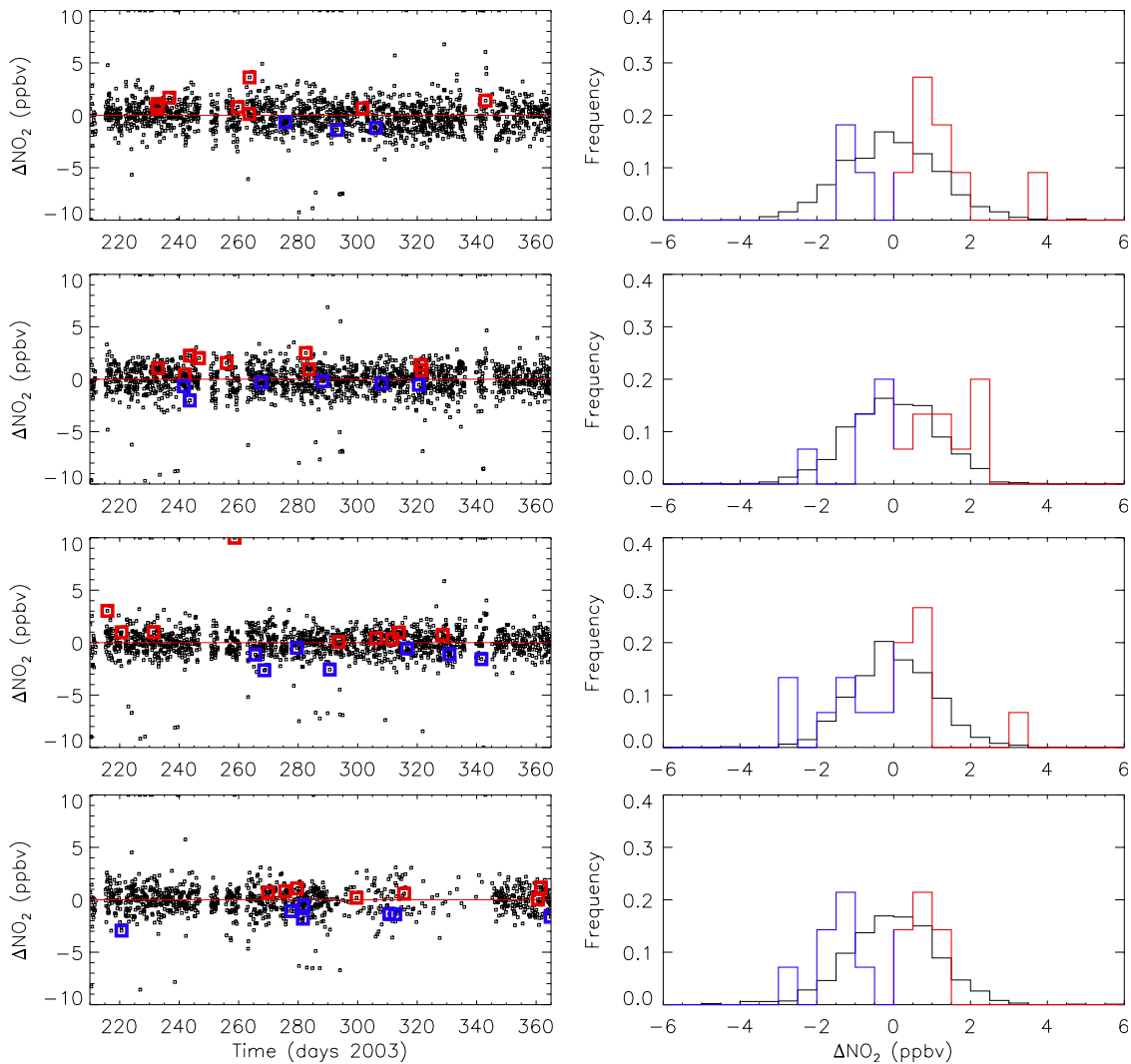
Figure 4. Left column—time series of MIPAS nighttime ΔNO_2 (black = background ΔNO_2, coloured = ΔNO_2 in coincidence with WWLLN lightning activity—WWLLN-NO_2, red for $\Delta > 0$ and blue for $\Delta < 0$) within $5°$ latitude bands and at 52 km height. The panels correspond to latitude bands from $20°N$–$15°N$, $10°N$–$5°N$, $5°N$–Equator and Equator–$5°$ (top to bottom). Right column—time-integrated distribution of ΔNO_2 corresponding to the respective panel in the left column (black = background NO_2 anomalies, red = WWLLN-$\Delta NO_2 > 0$, blue = WWLLN-$\Delta NO_2 < 0$).

the reference scenario. The distributions of the WWLLN-ΔNO_2 within these bands have a standard deviation between 1.2 and 1.6 ppbv. The northern two of these bands (panel 1 and panel 2 of the figure) have a mean value of +0.7 and +0.7 ppbv compared with those of the background (or median +0.8 and +0.9 compared with those of the background) which correspond to a shift of the distribution towards higher NO_2 values. The other two bands have a slightly negative or no shift (−0.3 and 0.0 ppbv, panels 3 and 4 from the top). A bootstrap (Efron 1979) statistical analysis showed that the risk of coincidence of the WWLLN-NO_2 and background NO_2 is non significant for the two positive displacements. The difference is thus statistically significant for the first and second panels, while it is insignificant for the other two.

All other latitude bands have four or fewer WWLLN-NO_2 and are thus statistically meaningless on their own. However, all anomalies were included in the subsequent analysis when discussing the dependence of all individual measurements on relevant parameters.

4.2. Discrimination of WWLLN-NO_2 against geolocation and time

The ΔNO_2 timeseries of figure 4 show that the northern bands (top panels) have a large majority of positive WWLLN-ΔNO_2 during about the first 6 weeks. This suggests the existence of a dependence of WWLLN-ΔNO_2 on geolocation and time. Figure 5 shows the distribution of WWLLN-ΔNO_2 versus latitude, longitude, time and lightning flash rate (top to bottom panels). The latter is discussed in the next section.

Positive WWLLN-ΔNO_2 do not show a clear correlation with latitude or longitude, although anomalies over northern bands are confirmed to have more positives (red squares) than negative (blue squares) values. The strongest selection appears to happen over time (third panel from the top): here the first 40–50 days (roughly up to day 270, 2003) are clearly dominated by positive ΔNO_2 (red dots) which in turn were identified to be in the northern bands. Comparing this selection with background zonal winds shown in figure 2, these anomalies

6
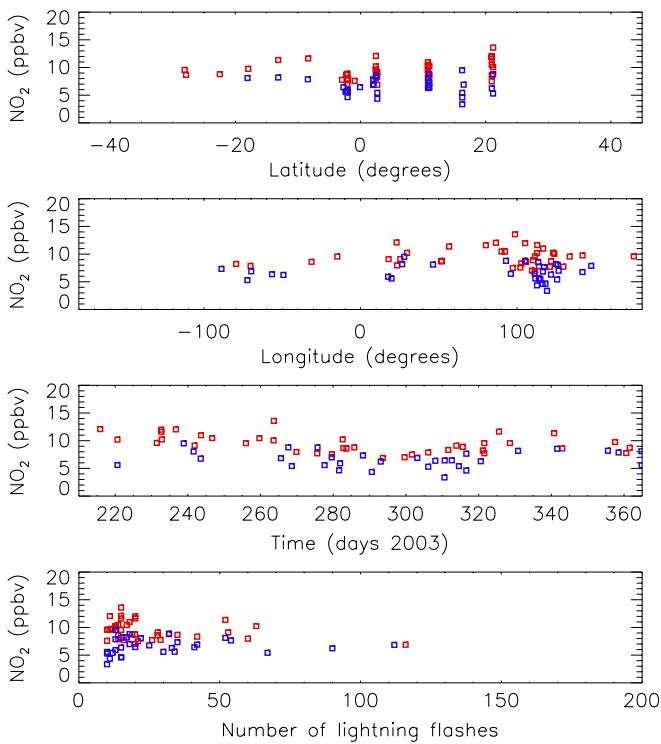
Figure 5. Sensitivity of the absolute value of WWLLN-NO$_2$ selected in the study to latitude, longitude, time and WWLLN lightning counts in the coincidence window (top to bottom). Red squares indicate positive anomalies and blue squares negative ones. See text for details.

overlap with a period of lower wind speeds (typically less than $20\,\mathrm{m\,s^{-1}}$): this is to be expected since slower transport and longer times of persistence of sprite-produced NO$_2$ above the location of emission makes MIPAS observations of actual sprite NO$_2$ more feasible. A further analysis of NO$_2$ anomalies and ECMWF data did not lead to a clear correlation between positive WWLLN-NO$_2$ and low winds over the whole dataset. A slight improvement was found in paper I by adopting backward trajectories based on ECMWF winds. However, if the correlation suggested in paper I exists, this is not strong enough to be statistically tested: the more likely higher-than-background values of the WWLLN-NO$_2$ over these regions is thus due also to larger local production rather than only to slower background winds.

WWLLN-NO$_2$ anomalies were also tested against biases introduced by the parameters of our analysis: we found no evidence of any significant correlation with the parameters of the retrieval (e.g. pressure, temperature, uncertainties). Only a very weak correlation with the retrieved water vapour at 52 km height was found and will be further investigated with a new extended MIPAS/GMTR dataset that has become available (the MIPAS2D database— http://www.mbf.fci.unibo.it/mipas2d.html).

4.3. Sensitivity to coincidence window and lightning count threshold

A number of tests were performed to analyse the sensitivity of the calculated WWLLN-ΔNO$_2$ to the size of the coincidence window, time interval and lightning threshold. The results showed consistency within a range of values of the adopted parameters. Increasing the coincidence window above a certain limit (roughly when counting more than twice as many coincidences as in the reference scenario), the WWLLN-NO$_2$ distribution tended to overlap with the background distribution (as expected). This was the case also with lowering the threshold on lightning to 1 WWLLN count. We also found that by adjusting the three parameters we could always find a range of parameter values that led to the same shape/size of the observed NO$_2$ enhancement so as to waive any possibility of randomness in the obtained results.

The correlation between WWLLN-NO$_2$ and lightning activity is shown in the bottom panel of figure 5. Unexpectedly, in regions of very high WWLLN lightning strokes count (>50 counts) the WWLLN-NO$_2$ is not dominated by positive anomalies and thus by enhancements in NO$_2$. This implies that even over extremely active regions, we cannot assume a direct correlation between high lightning activity (thus high likelihood of sprite activity) and high NO$_2$ on individual measurements, although a correlation exists over the overall sample. Further refinements to the adopted thunderstorm proxy are needed.

Finally, with all adopted scenarios we tested, the count of positive anomalies was always larger than the count of negative anomalies, further confirming a bias of WWLLN-NO$_2$ towards values higher than the background.

4.4. Non-physical NO$_2$ values

In our dataset a number of NO$_2$ values were discarded because of unphysically high values and associated errors. A further possible sprite signature may be found considering these anomalous values that the instrument may record in coincidence with very sharp NO$_2$ gradients that could be caused by TLEs. If the sprite-produced NO$_2$ VMR in one region deviated substantially from the values in adjacent regions or TLE-induced non-LTE deviations, the spectral fit may be very poor or the retrieval may fail returning non-physical NO$_2$ values.

We thus analysed the outliers and rejected data of the sample used in the investigation described above. We found that the number of NO$_2$ measurements rejected by our retrieval was about 1% of all available measurements in the range considered. Once the sample was restricted to MIPAS measurements in coincidence with intense lightning activity, the rejection rate rose to about 4%. Although the numbers considered are very small, we may be rejecting some measurements in coincidence with the strongest TLE activity.

The possibility of a failure of the retrieval in coincidence with sharp local gradients can be rejected because of the adoption of the GMTR two-dimensional retrieval: the adopted retrieval algorithm was shown to reproduce well sharp changes in NO$_2$, e.g. at the day–night terminator (see Carlotti *et al* (2006)). The retrieval failure may thus be due to temporary loss of local thermodynamic equilibrium with departure of vibrational or rotational temperatures from the kinetic temperature. In these cases, the retrieved absolute

VMR values may become meaningless, however, the time and geolocation of these measurements may be used as an indicator of anomalous processes such as TLEs.

As a first attempt to identify sprite-induced non-LTE emissions, we investigated the possible presence of enhanced radiation in the 4.3μm CO_2 line caused by the expected transfer of vibrational energy as discussed by Picard *et al* (1997). An enhancement of non-LTE emissions unexpected during nighttime would imply a direct measurement of sprite activity. We found no evidence of any such enhancements, mainly due to saturation of the 4.3μm CO_2 line and thus its limited sensitivity to small radiation enhancements. It should also be noted that the expected emission has timescales of 5–7 min, which would require exact time coincidence between satellite measurement and sprite occurrence, rather than the much more likely detection of the long persistent NO_2 perturbations as performed in this study.

4.5. Comparing models and observations

A comparison between model NO_x production within the streamer channel and satellite observations requires coupled sprite multi-streamer chemistry and chemical transport modelling to date unavailable. A first-order attempt at expanding from the sprite-streamer NO_x perturbation to local and global atmospheric scale was performed by Enell *et al* (2008). They suggested that during extremely intense sprite-producing thunderstorms (hundreds of sprites per hour), sprite-streamers might fill the whole volume above the thunderstorm so that the modelled streamer NO_x enhancements could be applied to the whole region. Based on their maximum production scenario, local perturbations would then range between a few to a few tens per cent above typical sprite-producing thunderstorms, and up to a few hundred per cent over extremely active ones, but with negligible global impact. Adopting these or their lower typical NO production estimates, the overall global production of NO_x is two to three orders of magnitude lower than other sources of NO_x in the stratosphere–mesosphere, namely oxidation of N_2O injected from the troposphere, solar particle precipitation and galactic cosmic rays (see Enell *et al* (2008) for details). If, on the other hand, one adopted the much larger (Hiraki *et al* 2008) estimates, sprites would become a significant component in the NO_x total budget.

The observational results we discussed suggest that higher-than-background NO_2 values in coincidence with thunderstorm activity are not as uncommon as the extraordinary cases discussed in Enell *et al* (2008), pointing to lower dilution or higher production than their standard case and thus to results closer to Hiraki *et al* (2008). Moreover, sprite activity after the time of MIPAS observations is expected to be stronger, so that our estimates might be a lower limit. However, due to the large unknowns present in performing such operations, most notably the *filling factor* (Enell *et al* 2008), i.e. the volume of a sprite which is actually filled by streamers, and the actual distribution of sprite-producing thunderstorms, constraints from the observations fail in clearly determining the correct estimates: even though

Hiraki *et al* (2008) estimates are much larger, they can be reconciled assuming different dilution factors. Moreover, our results are in line with both studies in showing an increasing magnitude of the perturbation (in per cent) with height as we found between 50 and 60 km height.

Considering both the modelling and our results, the expected production above thunderstorms can be significant. The lack of global signature we found on a 4-month-average (see figure 3 consistently with the results by Rodger *et al* (2008)) show that TLE are not the major source of NO_x. This may be misleading, however, if TLE are an important but not dominant source of NO_x due to the efficiency of zonal transport having timescales as short as days, as pointed out by Neubert *et al* (2008, chapter 10) using a first-order simulation in a transport model. Thus also a large contribution to the zonally averaged background NO_x cannot be ruled out as yet. Because of the modelled much smaller impact on ozone, direct perturbations to the radiative-dynamics equilibrium of the upper atmosphere can be ruled out. This was also discussed by Arnone *et al* (2008a) with a calculation of the maximum temperature change induced by expected maximum ozone changes of the order of 1%. In the unrealistic case of total absence of transport, they calculated a maximum temperature change of 0.3 K within the ozone-perturbed air localized above extraordinary sprite-producing thunderstorms, an impact which reduces to 0.015 K in typical cases, i.e. much smaller than natural variability.

It should be pointed out that given the relatively limited number of coincidences we found and the peculiarity of the NO_2 measurement at 10:00 pm which disregard a large fraction of sprites, extrapolations to global properties should be done with caution.

5. Conclusions

Sprite-induced NO_x signatures were investigated by studying nighttime satellite measurements of NO_2 at 50–60 km height in coincidence with thunderstorm activity. Sensitivity tests showed that the local enhancement in NO_2 of about +10% at 52 km height and tens of per cent at 60 km height in coincidence with intense lightning activity found in paper I is robust. The observational dataset was further investigated to trace back the regions and time periods giving the largest contribution.

Most of the higher-than-background NO_2 values in coincidence with thunderstorm activity are located north of the Equator and roughly during the first 6 weeks of our sample: this implies that the largest contribution to the observed enhancement is given by regions in late summer. Unfortunately, given the high variability of background NO_2 at mid-latitudes it was not possible to study the possible seasonal asymmetry between the summer and winter hemisphere. Moreover, the bias in the 2003 WWLLN detection efficiency and the different land/ocean ratio between the Northern and Southern Hemisphere may be favouring the coincidences of MIPAS observations with WWLLN lightning detections in the Northern Hemisphere.

Support for our finding also comes from the low sensitivity of the enhancement to the adopted coincidence windows. All

tested scenarios returned a higher fraction of positive NO_2 anomalies in coincidence with regions of high likelihood of sprite activity compared with negative anomalies. At a first-order level, it appears that NO_x enhancements are consistent with higher lightning activity (and possibly high sprite activity) in the summer tropics. These observational estimates indicate that sprite perturbations to middle atmospheric NO_2 may not be inconsistent with the minimum dilution/extraordinary case scenarios discussed by Enell *et al* (2008), thus suggesting very intense sprite-producing thunderstorms may be more frequent or have a larger local impact compared with their typical scenario. However, a more extended dataset is needed to further these first observations.

The availability of new MIPAS observations, the improvement of WWLLN detection efficiency after 2003 and use of cloud-top temperatures, and future dedicated missions such as the ASIM are expected to better define the distribution of sprite activity and that of sprite-induced perturbations, thus enhancing the possibility of finding coincidences between sprite-active regions and satellite measurements of NO_x. Given the crucial role of HO_x and NO_x in ozone chemistry, TLE contributions need to be better defined. The understanding of TLE-induced changes to the chemistry of the middle atmosphere may lead to using TLEs as a tool for investigating the properties of the hardly accessible middle atmosphere itself, thus supporting the need for further investigations.

Acknowledgments

References

Arnone E, Berg P, Arnold N F, Christiansen B and Thejll P 2008a An estimate of the impact of transient luminous events on the atmospheric temperature *Adv. Geosci.* **13** 37–43

Arnone E *et al* 2008b Seeking sprite-induced signatures in remotely sensed middle atmosphere NO_2 *Geophys. Res. Lett.* **35** 5807–+ doi:10.1029/2007GL031791

Barrington Leigh C P, Inan U S and Stanley M 2001 Identification of sprites and elves with intensified video and broadband array photometry *J. Geophys. Res.* **106** 1741–50

Brasseur G P and Solomon S 2005 *Aeronomy of the Middle Atmosphere* 3rd edn (Dordrecht: Springer)

Callis L B, Natarajan M and Lambeth J D 2002 Observed and calculated mesospheric NO 1992–1997 *Geophys. Res. Lett.* **29** 020,000–1 doi:10.1029/2001GL013995

Carlotti M, Dinelli B M, Raspollini P and Ridolfi M 2001 Geo-fit approach to the analysis of limb-scanning satellite measurements *Appl. Opt.* **40** 1872–85

Carlotti M, Brizzi G, Papandrea E, Prevedelli M, Ridolfi M, Dinelli B M and Magnani L 2006 GMTR: two-dimensional geo-fit multitarget retrieval model for Michelson Interferometer for passive atmospheric sounding/environmental satellite observations *Appl. Opt.* **45** 716–27

Chen A B *et al* 2008 Global distributions and occurrence rates of transient luminous events *J. Geophys. Res. (Space Phys.)* **113** 8306–+ doi:10.1029/2008JA013101

Christian H J *et al* 2003 Global frequency and distribution of lightning as observed from space by the optical transient detector *J. Geophys. Res. (Atmos.)* **108** 4005–+ doi:10.1029/2002JD002347

Efron B 1979 Bootstrap methods. Another look at the jackknife *Ann. Stat.* **7** 1–26

Enell C-F *et al* 2008 Parameterisation of the chemical effect of sprites in the middle atmosphere *Ann. Geophys.* **26** 13–27

Fischer H *et al* 2008 MIPAS: an instrument for atmospheric and climate research *Atmos. Chem. Phys.* **8** 2151–88

Fukunishi H, Takahashi Y, Kubota M and Sakanoi K 1996 Elves: lightning induced transient luminous events in the lower ionosphere *Geophys. Res. Lett.* **23** 2157

Füllekrug M, Mareev E A and Rycroft M J (ed.) 2006 *Sprites, Elves and Intense Lightning Discharges* (*NATO Science Series II. Mathematics, Physics and Chemistry* vol 225) (Berlin: Springer) ISBN 1-4020-4628-6

Funke B, López-Puertas M, Gil-López S, von Clarmann T, Stiller G P, Fischer H and Kellmann S 2005a Downward transport of upper atmospheric NO_x into the polar stratosphere and lower mesosphere during the Antarctic 2003 and Arctic 2002/2003 winters *J. Geophys. Res. (Atmos.)* **110** 24.308–+ doi:10.1029/2005JD006463

Funke B *et al* 2005b Retrieval of stratospheric NO_x from 5.3 and 6.2 μm nonlocal thermodynamic equilibrium emissions measured by Michelson Interferometer for Passive Atmospheric Sounding (MIPAS) on Envisat *J. Geophys. Res. (Atmos.)* **110** 9302–+ doi:10.1029/2004JD005225

Gordillo-Vázquez F 2008 Air plasma kinetics under the influence of sprites *J. Phys. D: Appl. Phys.* **41** 234.016

Hiraki Y, Kasai Y and Fukunishi H 2008 Chemistry of sprite discharges through ion-neutral reactions *Atmos. Chem. Phys.* **8** 3919–28

Jacobson A R, Holzworth R, Harlin J, Dowden R and Lay E 2006 Performance assessment of the World Wide Lightning Location Network (WWLLN), using the Los Alamos Sferic Array (LASA) as Ground Truth *J. Atmos. Ocean. Technol.* **A-731**

Krehbiel P R, Riousset J A, Pasko V P, Thomas R J, Rison W, Stanley M A and Edens H E 2008 Upward electrical discharges from thunderstorms *Nature Geosci.* **1** 233–7

Lyons W A 2006 The meteorology of transient luminous events—an introduction and overview *Sprites, Elves and Intense Lightning Discharges* (*NATO Science Series II. Mathematics, Physics and Chemistry* vol 225) ed M Füllekrug *et al* (Berlin: Springer) ISBN 1-4020-4628-6 pp 19–56

McHarg M G, Stenbaek-Nielsen H C and Kammae T 2007 Observations of streamer formation in sprites **34** 6804–+ doi:10.1029/2006GL027854

Neubert T *et al* 2008 Recent results from studies of electrical discharges in the mesosphere *Surv. Geophys.* submitted doi:10.1007/s10712-008-9043-1

Pasko V P 2007 Topical Review: red sprite discharges in the atmosphere at high altitude: the molecular physics and the similarity with laboratory discharges *Plasma Sources Sci. Technol.* **16** 13–+ doi:10.1088/0963-0252/16/1/S02

Pasko V P, Inan U S, Bell T F and Taranenko Y N 1997 Sprites produced by quasi-electrostatic heating and ionization in the lower ionosphere *J. Geophys. Res.* **102** 4529–61

Pasko V P, Inan U S and Bell T F 1998 Spatial structure of sprites *Geophys. Res. Lett.* **25** 2123–6

Pasko V P, Stanley M A, Mathews J D, Inan U S and Wood T G 2002 Electrical discharge from a thundercloud top to the lower ionosphere *Nature* **416** 152–4

Picard R H, Inan U S, Pasko V P, Winick J R and Wintersteiner P P 1997 Infrared glow above thunderstorms? *Geophys. Res. Lett.* **24** 2635–8

Rodger C J 1999 Red sprites, upward lightning, and VLF perturbations *Rev. Geophys.* **37** 317–36

Rodger C J, Werner S, Brundell J, Thomson E, Lay N R, Holzworth R and Dowden R 2006 Detection efficiency of the VLF World-Wide Lightning Location Network (WWLLN): initial case study *Ann. Geophys.* **24** 3197–214

Rodger C J, Seppälä A and Clilverd M A 2008 Significance of transient luminous events to neutral chemistry: experimental measurements *Geophys. Res. Lett.* **35** 1–5

São Sabbas F T and Sentman D D 2003 Dynamical relationship of infrared cloudtop temperatures with occurrence rates of cloud-to-ground lightning and sprites *Geophys. Res. Lett.* **30** 050,000–1 doi:10.1029/2002GL015382

Sentman D D, Wescott E M, Osborne D L, Hampton D L and Heavner M J 1995 Preliminary results from the Sprites94 aircraft campaign: I. Red sprites *Geophys. Res. Lett.* **22** 1205–8

Sentman D D, Stenbaek-Nielsen H C, McHarg M G and Morrill J S 2008 Plasma chemistry of sprite streamers *J. Geophys. Res. (Atmos.)* **113** 1–33

Seppälä A, Clilverd M A and Rodger C J 2007 NO_x enhancements in the middle atmosphere during 2003–2004 polar winter: relative significance of solar proton events and the aurora as a source *J. Geophys. Res. (Atmos.)* **112** 23.303–+ doi:10.1029/2006JD008326

Wescott E M, Sentman D, Osborne D, Hampton D and Heavner M 1995 Preliminary results from the Sprites94 aircraft campaign: II. Blue jets, *Geophys. Res. Lett.* **22** 1209–12

Williams E R 1992 The Schumann resonance: a global tropical thermometer *Science* **256** 1184–7 doi:10.1126/science.256.5060.1184